Electrospinning of *p*-Aramid Fibers

Jian Yao, Junhong Jin, Emiliano Lepore, Nicola M. Pugno, Cees W.M. Bastiaansen, Ton Peijs*

Electrospun poly (*p*-phenylene terephthalamide) (PPTA) fibers with diameters between 275 nm and 15 μm were obtained from anisotropic solutions, albeit that the spinning process was difficult to control. Key solution parameters like conductivity, surface tension, and viscosity were used to compare the spinnability of these anisotropic solutions with common polymer solutions in order to better understand the challenges of spinning such solutions. Mechanical properties of the electrospun *p*-aramid single fibers were evaluated and it was found that Young's modulus and tensile strength increased dramatically with decreasing fiber diameter. A maximum Young's modulus and tensile strength of 59 and 1.1 GPa, respectively were found and a geometrical model for the size-dependent Young's modulus was developed to predict fiber properties based on rigid-rod chains down to the nanoscale.

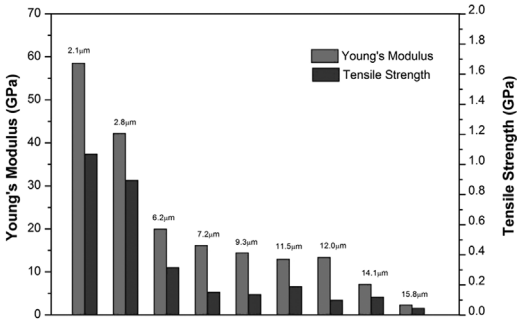

1. Introduction

In order to create high-strength and high-modulus fibers, it is vital to achieve chain orientation and chain extension along the fiber axis.[1] In the case of electrospun fibers, mechanical properties are often found to be poor compared to corresponding synthetic textile fibers made from the same polymers due to their low degree of chain orientation and chain extension. Orientation of macromolecules can be introduced when the product of polymer chain relaxation time and the extension rate in the electrospinning process is greater than 0.5.[2] Given the fact that the relaxation time of flexible chain polymers is typically very short, orientation induced in the initial spinning process can rapidly disappear due to relaxation before solidification.[3] It is for this reason that high-performance fibers based on flexible chain polymers are typically post-drawn in the solid state below the melting temperature, where relaxation times are nearly infinite. However, such an approach is usually not feasible in electrospinning due to technological difficulties with respect to the post-drawing of nanosized fibers.[4] Only limited stretching or drawing has been attempted to aligned nanofiber mats in order to induce some levels of molecular orientation and crystallinity, which often remained rather low.[5]

An alternative approach to achieve high levels of chain orientation and chain extension is through the use of rigid rod polymers. The main reason to use rigid rod polymers is that in these systems, chain extension is already built in by the chemist whilst flow-induced chain orientation of such rigid rods can be induced during the spinning process. *p*-Aramid fiber is the prime example of a high–performance,

Dr. J. Yao, Prof. N. M. Pugno, Prof. C. W. M. Bastiaansen, Prof. T. Peijs
School of Engineering and Materials Science, and Materials Research Institute, Queen Mary University of London, Mile End Road, London E1 4NS, UK
Dr. J. Jin
State Key Laboratory for Modification of Chemical Fibers and Polymer Materials, College of Material Science and Engineering, Donghua University, Shanghai 201620, PR China
Dr. E. Lepore, Prof. N. M. Pugno
Laboratory of Bio-Inspired and Graphene Nanomechanics, Department of Civil, Environmental and Mechanical Engineering, University of Trento, Via Mesiano 77 38123, Trento, Italy
Prof. C. W. M. Bastiaansen
Faculty of Chemistry and Chemical Engineering, Eindhoven University of Technology, P.O. Box 513, 5600 MB, Eindhoven, The Netherlands
Prof. T. Peijs
Nanoforce Technology Ltd., Joseph Priestly Building, Queen Mary University of London, Mile End Road, London E1 4NS, UK
E-mail: t.peijs@qmul.ac.uk
Prof. N. M. Pugno
Centre for Materials and Microsystems, Fondazione Bruno Kessler, Via Sommarive 18 I-38123, Trento, Italy

DOI: 10.1002/mame.201500130

synthetic fibers spun from rigid (or semi-rigid) polymer chains. When PPTA is dissolved in concentrated sulfuric acid at low concentration, the rigid rod molecules are randomly distributed in the isotropic phase. These rod-like molecules will tend to arrange themselves to form nematic domains above a certain concentration. Furthermore, they can be oriented in the fiber direction when they are subjected to elongational flow during spinning.[6] Using such an approach, conventional high-performance *p*-aramid fibers have been produced using dry-jet wet spinning technologies taking advantage of the anisotropic properties of PPTA solutions.[7]

Great success has been achieved by developing through these routes high-performance *p*-aramid fibers like Kevlar and Twaron with typical fiber diameters of around 14 μm.[8] However, until recently few efforts were devoted to the development of electrospun *p*-aramid nanofibers. Reneker and co-workers[9] attempted to electrospin 2–3 wt% of PPTA solutions from the isotropic phase. Although nanoscale fibers were obtained, no mechanical properties were reported. Unfortunately, the concentrations of these spinnable solutions were well outside the anisotropic regime (19–20 wt%) needed for high-performance *p*-aramid fibers, which implies that mechanical properties of these fibers would have been rather poor.

In this work, we aim to develop high-performance PPTA nanofibers by electrospinning anisotropic solutions. First, the electro-spinnability of both isotropic and anisotropic PPTA solutions is investigated. Subsequently, the need for using relatively high voltages in the electrospinning of these materials is analyzed followed with a discussion on the difficulties and challenges in creating a continuous and technologically feasible electrospinning process for PPTA. Finally, the mechanical properties of the *p*-aramid fibers obtained from the above process are discussed and correlated to their size effects.

2. Experimental Section

2.1. Solution Preparation and Electrospinning

98 wt% of concentrated sulfuric acid was prepared by diluting fuming sulfuric acid containing 20% sulfur trioxide (purchased from Sigma–Aldrich) with distilled water. For instance, in order to make 98 wt% of sulfuric acid, 100 g fuming sulfuric containing 20 g of sulfur trioxide needs to be added with 6.59 g of distilled water.

A 19.46 wt% PPTA in concentrated sulfuric acid solution (kindly provided by Teijin Aramid, The Netherlands) was diluted to produce three isotropic solutions of 2, 5, and 7 wt% and two anisotropic solutions of 15 and 17 wt% by adding 98 wt% of sulfuric acid. All solutions were prepared using mild stirring in an oil bath at 85 °C for 3 h.

In the electrospinning process, voltages between 0 and 30 kV were employed, distances from 8 to 2 cm and flow rates between 0.2 and 2 ml h^{-1} were adjusted to obtain fibers. A water bath was used to coagulate and collect the fibers. Moreover, a heating band was used to maintain the temperature of the spinning solutions between 80 and 90 °C.

2.2. Tensile Testing and Fiber Characterization

The resulting electrospun fibers were tested using a micro-tensile tester (Agilent T150 UTM, load resolution of 50 nN).[10] As shown in Figure 1, single fibers were mounted on a paper frame with a fixed internal dimension of 10×5 mm^2. Super glue and double-sided tapes were used to fix the single fibers to the frame and no clamp slippage was observed during testing. The strain rate during tensile testing was 0.1 mm s^{-1}. Samples that failed close to or inside the grip were discarded.

Morphological studies of the fibers were performed using a scanning electron microscope (FEI, Inspect F). All of the samples were gold coated before observation.

3. Results and Discussion

3.1. Electrospinning from Isotropic and Anisotropic PPTA Solutions

The relation of viscosity as a function of concentration of moderate molecular weight PPTA in sulfuric acid above 80 °C was presented in our previous report.[1] An increase in solution concentration results in an increase in viscosity in the isotropic phase when PPTA molecules are randomly aligned. For this reason, PPTA solutions are considered to be in their isotropic phase at low concentrations (typically $<$ 12 wt%). The viscosity reduces sharply at a critical concentration with a further increase in solution concentration due to the self-assembly of molecules into nematic liquid crystal domains until the viscosity reaches a minimum at a concentration of around 20 wt% when the solution becomes fully liquid crystalline. Above this concentration, the solution viscosity will increase again with the appearance of a PPTA solid phase caused by the super-saturation of the solution. Conventional *p*-aramid fibers are therefore spun from solution concentrations of around 20 wt%, i.e., around the minimum viscosity and taking advantage of the anisotropic properties of PPTA solutions.[11]

A typical electrospinning set-up is shown in Figure 2. It should be noted that these anisotropic PPTA solutions are biphasic with both nematic phase and solid phase below

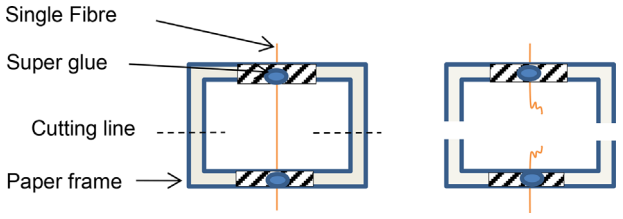

Figure 1. Schematic illustration of single fiber sample preparation for mechanical tests.

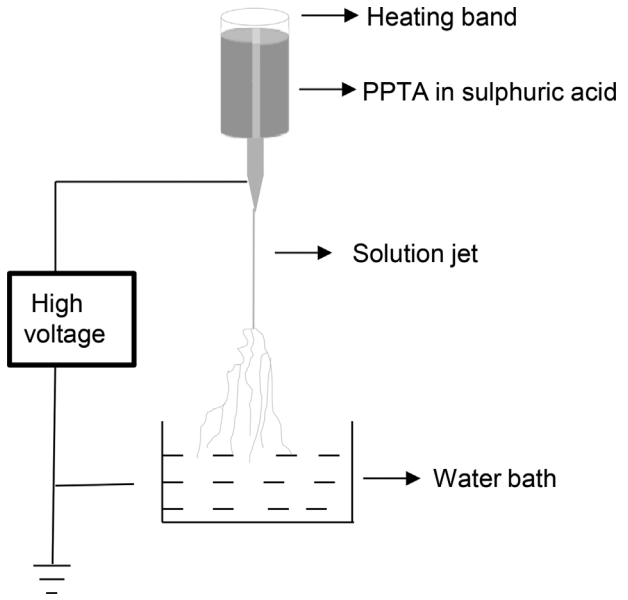

Figure 2. Schematic illustration of electrospinning set-up of PPTA in concentrated sulfuric acid solutions.

80 °C while degradation of PPTA occurs above 90 °C. Hence, a heating band with a precise temperature control system to the syringe is necessary to ensure a spinning solution temperature of 85 °C.

Electrospinning involves charging the spinning solution using high voltage and consequently a solution jet could eject from the pending droplet on the nozzle when its surface tension is overcome by the electrostatic repulsion forces. In this work, spinning parameters such as applied voltage, distance, and flow rate of solution were adjusted to make the solution spinnable. It should be noted that a water bath is needed as a collector to extract the solvent and coagulate the solution jets into fibers because of the non-volatile property of sulfuric acid. Subsequently, those fibers are transported for drying at 60 °C overnight. It is important to know that the spinning solution jet in this work is relatively straight and few whipping instabilities were observed due to the use of high voltages and short spinning distances. Branched solution jets were found close to the coagulation bath, which will be discussed in the next section.

The spinnability of the PPTA solutions is of primary importance for the technological feasibility of electrospun PPTA fibers. In the case of electrospinning of isotropic solutions, only small and large droplets were deposited in the coagulation bath for 3 and 5 wt% solutions, respectively. After washing and drying, these droplet morphologies are shown in Figure 3a and b, respectively. With increasing solution concentration, short fibers (lengths $< 100\ \mu m$) of varying diameters (2–20 μm) were collected from the 7 wt% solution at an applied voltage of 25 kV and a distance of 5 cm, as shown in Figure 3c. Further increase of solution

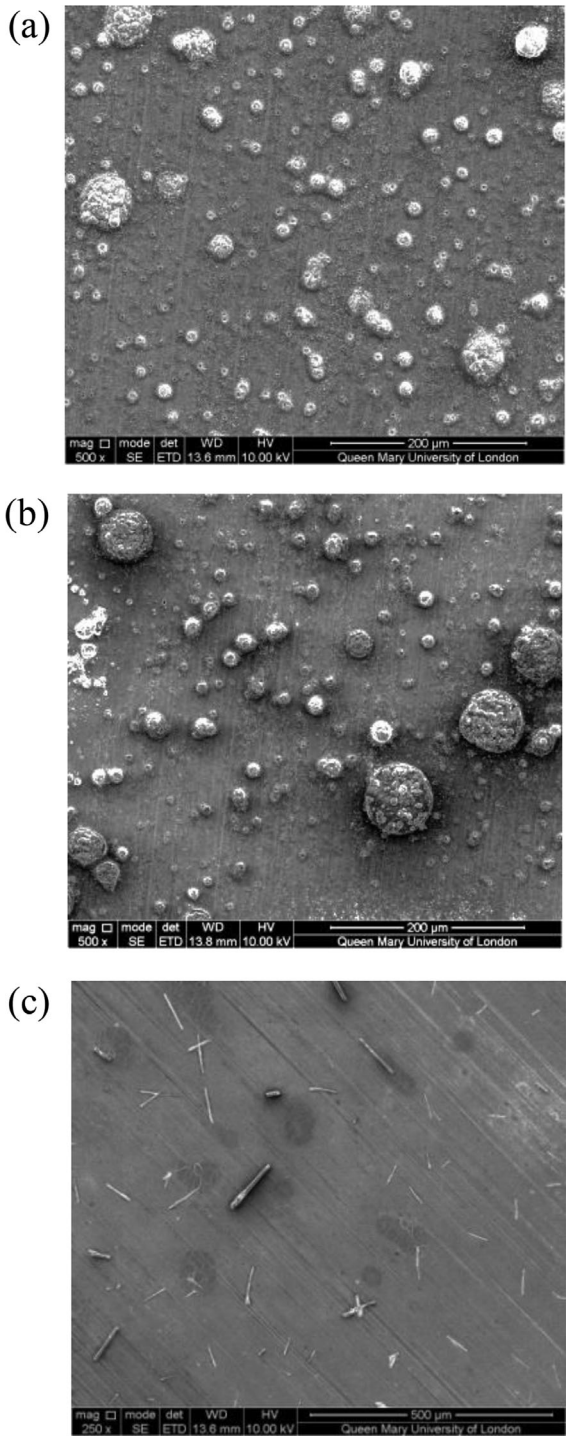

Figure 3. SEM micrographs of electrospun (or rather electrosprayed) PPTA solutions with concentrations of (a) 3 wt% (b) 5 wt%, and (c) 7 wt% PPTA in H_2SO_4.

concentration lead to a rapid increase in viscosity of spinning solution but failed to result to longer fibers.

This phenomenon can be ascribed to the fact that the surface tension of solution dominates the

electrospinning process at low concentrations, hence leading to the formation of droplets or stretched droplets (short fibers).[12] Meanwhile, due to the non-volatility of sulfuric acid, no solid fibers were obtained before the coagulation bath. During the spinning process, the solution jet is prone to break when it is stretched due to the absence of chain entanglements in the low-concentration solutions. Therefore, under these circumstances, the process can be considered to be electrospraying rather than electrospinning.

With respect to the electrospinning of anisotropic solutions, the solvent molecules have a tendency to interact with polymer molecules rather than congregate together, which is attributed to the highly concentrated solution. Consequently, the solution jet is stretched and fibers can be obtained without breakage of the jet owing to a sufficient level of viscoelasticity of the solution. The *p*-aramid fibers electrospun from 15, 17, and 19.46 wt% of anisotropic solutions are shown in Figure 4(a, b, c). A broad range of fiber diameters from about 300 to 16 μm were found for all of the three anisotropic spinning solutions.

3.2. Feasibility of Electrospinning Conditions for *p*-Aramid Fibers

It should be noted that the electrospinning parameters (spinning voltage, distance, flowing rate, etc.) needed in this work to obtain fibers all varied within narrow ranges. Specifically, electric field strength (4 kV cm^{-1}) used was about threefold of that of normal electrospinning.[2] Low electric field strength leads to greater tendency of droplet formation, while too high electric field strength is prone to give rise to corona discharge. In both situations, no fibers will be obtained. Here, the electrospinning of anisotropic PPTA solutions (15, 17, and 19.46 wt%) gave similar fiber diameter distributions, as shown in Figure 4 (a, b, and c).

Three key solution parameters are listed in Table 1 which can significantly influence the processing parameters, i.e., applied voltage or potential electrical field. Compared to other commonly used electrospinning solvents, the conductivity of solvent used in this study is significantly higher. Meanwhile, the essential difference of the anisotropic PPTA solution with other common electrospinning solutions is the relatively high solution viscosity, as shown in Table 1. Although the surface tension of 98% sulfuric acid is of the same order as surface tensions measured for common electrospinning solutions, it is not directly comparable as the surface tension of the anisotropic PPTA solution is unknown, it can still be concluded that high voltages are needed to generate sufficient electrostatic forces to stretch the electrospinning jet into micro-scale or nanoscale fibers in the case of these anisotropic PPTA solutions. The necessity of high voltage is not due to the conductivity of the solution but mainly the result of the high viscosities of PPTA solutions. In order to better understand the role of applied high voltage (or high electrical field) in the process, a similar set-up without applied voltage was used to produce fibers from the same

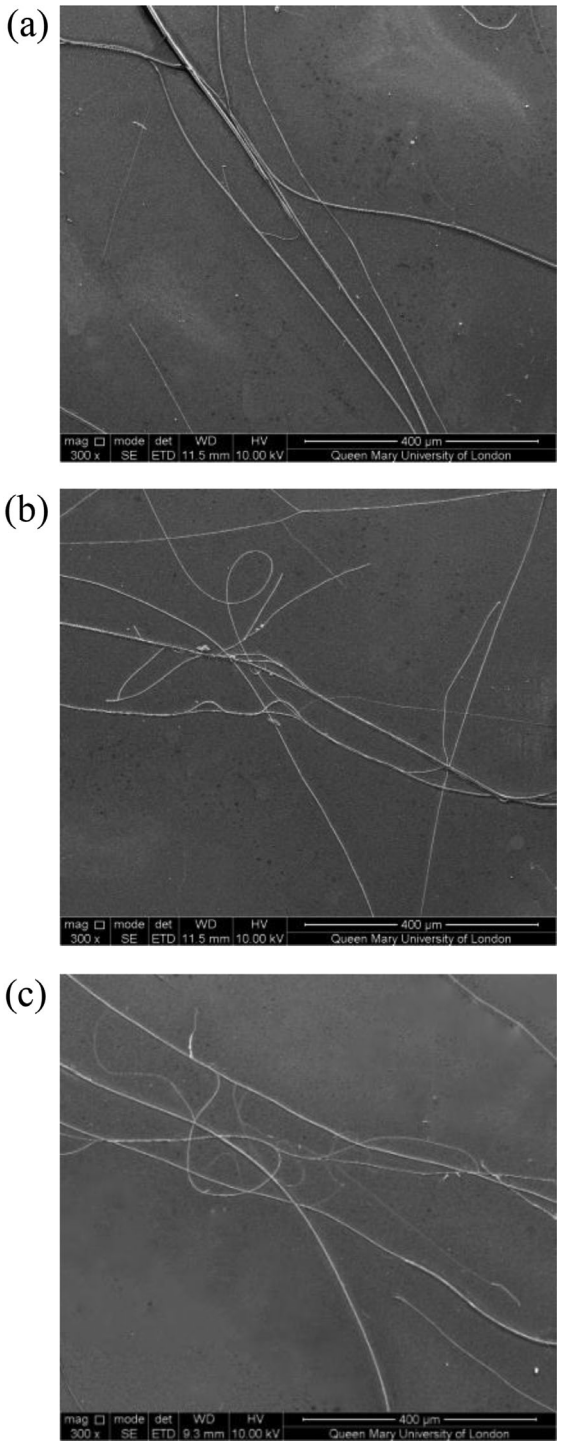

Figure 4. SEM micrographs of fibers electrospun from PPTA solutions with concentrations of (a) 15 wt% (b) 17 wt%, and (c) 19.46 wt% PPTA in H_2SO_4.

Table 1. Viscosity, conductivity, and surface tension of anisotropic PPTA solutions compared with common polymer solutions employed in electrospinning.

Solutions	Viscosity [1×10^3 cP]	Conductivity of solvents [mS m^{-1}]	Surface tension [mN m]	Ref.
Anisotropic PPTA solutions	650–1000	73.5–83.5 (80–90°C)	≈55 (98% H_2SO_4)	[13]
Common electrospun polymer solutions	0.02–300	0.05–30 (RT)	20–75	[14]

lyotropic solutions. It was found that large fibers with diameters varying from 2 mm to 50 μm can be collected. Mechanical properties of these fibers were found to be inferior to the largest diameter electrospun fibers collected with applied voltage, as will be shown in the next section. As such, this reference experiment indicated that an applied voltage is essential to fabricate thin fibers and to induce alignment of the PPTA molecules in the fibers.

Nevertheless, two significant phenomena arise with the application of high electrical field strengths. First of all, abundant branching was observed, as shown in Figure 4. This is because the solution jet is easily disturbed by the high voltage, and the high-density charges tend to build up in the solution jet as a result of the high electric field. As a result, several secondary jets are formed from the primary jet during spinning in order to reduce the local charges per unit surface area,[3] leading eventually to branched fibers. Fibers with diameters ranging from 16 μm to hundreds of nanometers can be found in the deposited fiber branches and it was impossible to control the fiber diameter within a certain range independent of spinning parameters. Also fibers with diameters less than 2 μm rarely had a length above 3 mm, which makes them difficult to test but also have implications for potential applications. Branched solution jets did, however, lead to nanoscaled electrospun PPTA fibers.

Secondly, it is worth reminding that the electrospinning process in this work could not be operated in a controllable and continuous manner which is once again mainly attributed to the high voltage caused solution jets breakage. Therefore, continuous electrospinning was not realized in this work and a large quantities of electrospun *p*-aramid fiber could not be collected. Nevertheless, sufficient amounts of PPTA fibers could be collected to access their mechanical performance.

3.3. Mechanical Properties of Electrospun *p*-Aramid Fibers

Conventional *p*-aramid fiber is regarded as one of the most important high-performance fibers with high stiffness and tensile strength (Young's modulus >60 GPa and tensile strength >2 GPa).

With respect to the electrospun *p*-aramid fibers reported here, an obvious birefringence can be observed under crossed polarizers, as shown in Figure 5, which indicates that alignment of liquid crystals is induced in the *p*-aramid fibers during electrospinning. As mentioned above, the electrospinning of PPTA resulted in branched fibers with a wide distribution in fiber diameters. Mechanical properties of this wide range of fiber diameters were evaluated in order to study possible size effects. Single electrospun *p*-aramid fibers were carefully separated from the coagulated and

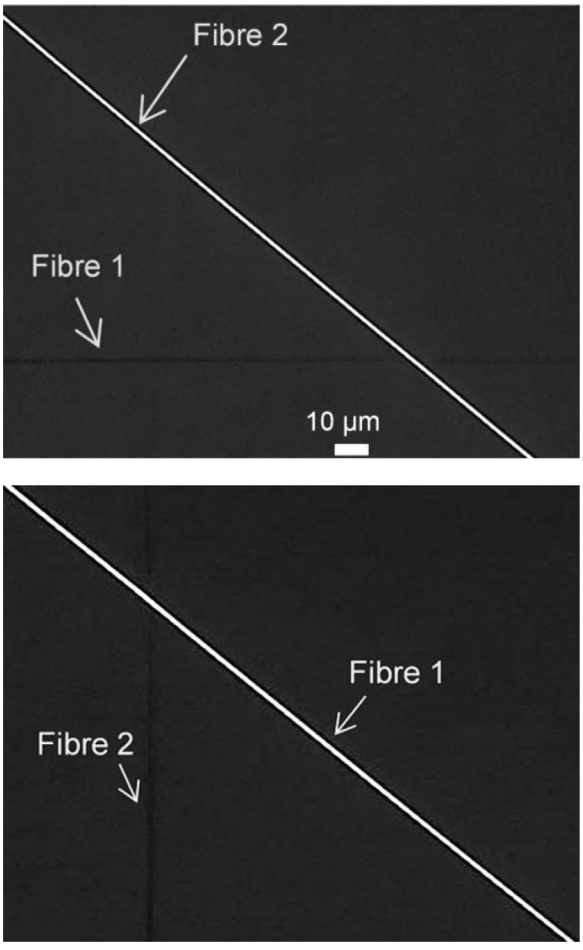

Figure 5. Electrospun *p*-aramid fibers from 19.46 wt% anisotropic solution under crossed polarizer (a) fiber 1 is positioned parallel with one piece of polarizer, whilst fiber 2 is positioned at a 45° angle with the polarizer (b) after 45° clockwise rotation of sample stage.

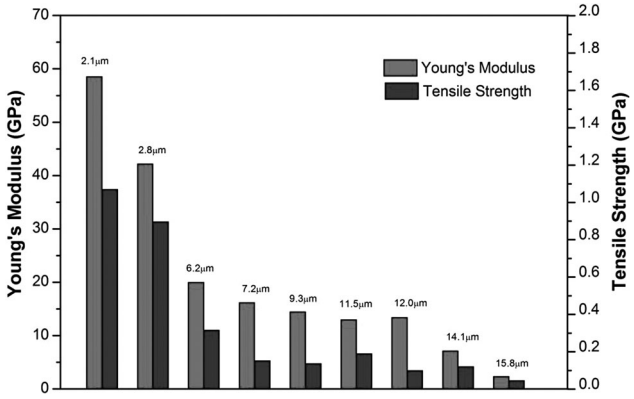

Figure 6. Tensile strength and Young's modulus of electrospun PPTA fibers with varying fiber diameter.

dried fiber bundles and glued to the prepared paper frame, as shown in Figure 1 for tensile testing. Figure 6 and 7 shows that the Young's modulus and tensile strength of tested single fibers increased with decreasing fiber diameter, clearly indicating a significant diameter effect. Size effects on the mechanical properties of electrospun fibers have been studied extensively for flexible chain polymers.[15] Many studies showed that decreasing the nanofiber diameter can effectively enhance the Young's modulus of these nanofibers and is often ascribed to confinement of polymer coils forcing them to align to some extent along the fiber axis, hence leading to improvement of molecular orientation and crystallinity,[5] as well as orientation of amorphous regions when their sizes are comparable or larger than the nanofibre diameter.[16] Compared to flexible chain bulk polymers, the Young's moduli of electrospun nanofibers can show a several folds (typically 2–4) increase with decreasing fiber diameter, but these improvements are relatively small compared to improvements (typically

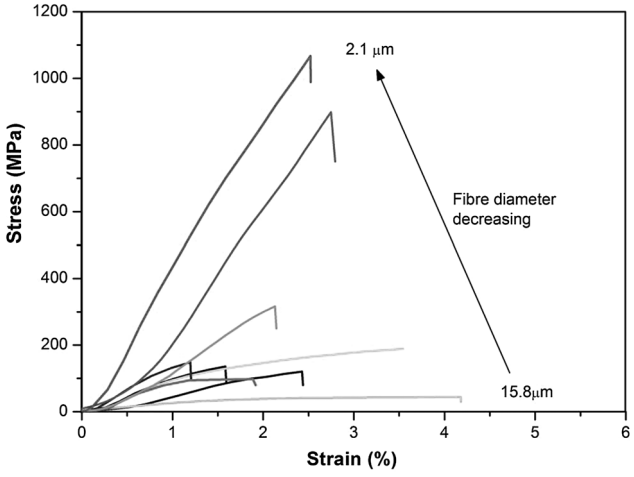

Figure 7. Stress–strain curves of electrospun PPTA fibers with different diameters.

10–100) observed in super-drawn, high-performance polymer fibers.[17] Full chain extension as observed in super-drawn, high-performance fibers is not achieved in these fibers mainly due to the absence of a subsequent solid-state drawing process in the of as-spun nanofibers based on flexible chain polymers.

As mentioned before, rigid chain polymers have a significant advantage over flexible chain polymers for the creation of high-performance electrospun fibers as these systems can be oriented during the spinning process without the need of a post-drawing process to induce high levels of chain extension as chain extension is already built in by the polymer chemist.[1] In our electrospinning work, *p*-aramid fibers are fabricated from high elongation flows where PPTA molecules are forced to align along the fiber axis. As a result, high levels of chain orientation and chain extension are achieved in these as-spun fibers without the need of post-drawing. However, it is also expected that thinner fibers would experience higher levels of elongational flow and better molecular orientation, leading to higher mechanical properties. For the PPTA system, a 20-fold increase in Young's modulus is seen with decreasing fiber diameter. This diameter effect is far greater than values typically reported for electrospun nanofibers based on flexible chain polymers (typically 2–4),[1] and highlights the potential of rigid rod polymers to create high-performance electrospun nanofibers.

In comparison to commercial *p*-aramid fibers, the highest Young's modulus value of 59 GPa measured for a fiber with a diameter of 2.1 μm is relatively low but is similar or approaches values of Standard Twaron 1000 or Kevlar 29 fibers (60–80 GPa[17]). It is also interesting to mention here that nanofibers of several hundred nanometers have been produced based on Teijin's proprietary Teijin conex *m*-aramid, which is a less rigid molecule than *p*-aramid. Although no further data are reported for these *m*-aramid nanofibers, their mechanical properties are expected to be at best similar to conventional *m*-aramid fibers (modulus <12 GPa; strength <600 MPa) and well below those reported in our study. *Meta*-aramid fibers are mainly used for flame-resistant technical textile applications rather than for applications requiring high mechanical properties.

Northolt et al. developed a detailed mathematic model to describe the relation between fiber compliance and chain orientation distribution on the basis of a single-phase crystalline model for the microstructure of PPTA fibers[18]

$$S = \frac{1}{e} + A < \sin^2\vartheta > \quad (1)$$

where S is the fiber compliance, e represents the theoretical modulus when the molecular chains are parallel to the fiber axis and $< \sin^2\vartheta >$ represents the chain orientation distribution with the fiber axis and A is a factor representing

the mechanical anisotropy of the crystallite. This equation has been verified experimentally by Northolt for PPTA fibers and it was shown that the fiber compliance corresponds linearly with the chain orientation distribution.[18a]

On the basis of Equation (1), the Young's modulus of the as-spun fiber is therefore expected to scale as $(1/E) \propto (1 - \cos^2\vartheta)$ where $\cos^2\vartheta$ is derived from $< \sin^2\vartheta >$ as the chains mean orientation after spinning and E is the Young's modulus of fiber which can be ascribed as the reciprocal of the fiber compliance. During spinning, the chains within the fiber become more aligned as a consequence of the geometrical diameter reduction. Assuming the spinning material is incompressible, we geometrically find $\tan\vartheta(r) = (r/R)^{\omega}\tan\vartheta(R)$. Note that for a constant volume under small elastic deformations, which is not the case for large plastic deformations as during spinning, the Poisson's ratio is $\nu = 1/2$; while the other limiting case of $\nu = 0$ denotes maximal compressibility and, for such a case, we find the same scaling but with the exponent $\omega = 1$. For our case, we expect an intermediate value of $1 \leq \omega \leq 2$.

The Young's modulus therefore should scale as follows:

$$\frac{1}{E} = \frac{1}{e} + A < 1 - \cos^2\vartheta > = \frac{1}{e} + A\left(1 - \frac{1}{1 + \tan^2\vartheta(R)\left(\frac{r}{R}\right)^{2w}}\right) \quad (2)$$

where e is considered to be about 160 GPa which is the theoretical modulus of PPTA.[1]

If three sets of data ($r = 2.1$ μm, $E = 58$ GPa; $R = 2.8$ μm, $E = 42$ GPa; $r = 6.2$ μm, $E = 20$ GPa) were fitted with Equation (3), the values of A, w, and $\tan\theta$ are 0.055, 0.126, and 0.718, respectively.

Then, one set of data ($R = 2.8$ μm, $E = 42$ GPa) was selected to be fitted with Equation (2), and is written as follows:

$$\frac{1}{E} = \frac{1}{156} + 0.055\left(1 - \frac{1}{1 + 0.72^2\left(\frac{r}{2.8}\right)^{2.526}}\right) \quad (3)$$

An "S"-shaped curve is predicted, as shown in Figure 8 based on Equation (3). Most of the experimental data are clearly well fitted by the model with little deviation. More importantly, although fibers with diameter less than 2 μm are difficult to test due to their short lengths (< 3 mm), the Young's modulus of these fibers can now be estimated from the curve with an ultimate stiffness of 160 GPa when all PPTA molecules are perfectly aligned ($\tan\theta = 0$). For example, in our branched electrospun fibers, PPTA filaments with diameters as low as 250 nm were observed but could not be tested. However, based on the above geometrical model, such fibers are predicted to have Young's moduli of around 150 GPa, approaching the theoretical modulus of PPTA, and exceeding moduli of commercial High Modulus Twaron or Kevlar 49 fibers (125 GPa).

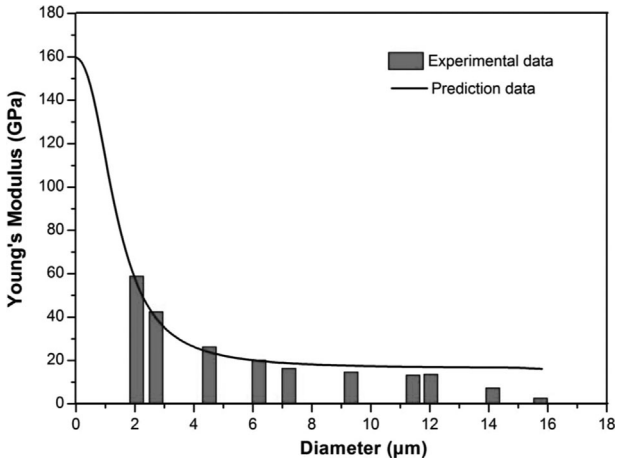

Figure 8. Experimental Young's modulus of electrospun PPTA fibers and prediction based on Equation (2).

An obvious shortcoming of the electrospun fibers reported in this work is their relatively low tensile strengths compared to conventional *p*-aramid fibers. The maximum tensile strength achieved is about 1.1 GPa and although these values are among the highest reported for electrospun fibers, they are only half those of commercial *p*-aramid fibers. Given the fact that tensile strength of fibers is sensitive to defects, any possible flaw (Figure 9) induced from the electrospinning process, coagulation, or handling of the fibers causing kinking can be detrimental to the final tensile strengths. Because of this, it is not surprising that strengths of fibers produced under non-optimal conditions as in this work are well below those of fibers spun under fully optimized commercial spinning conditions.

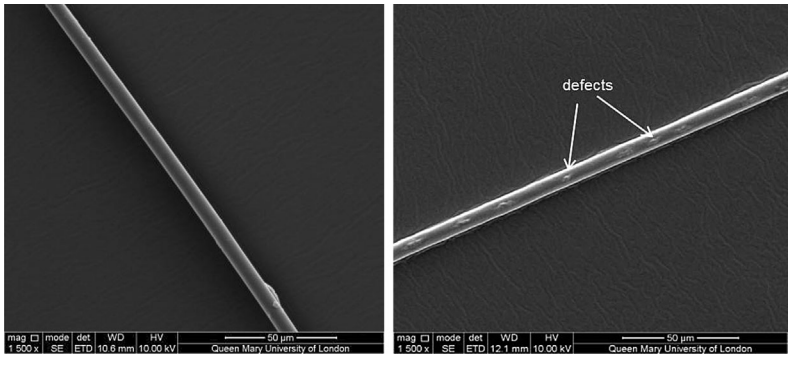

Figure 9. Comparison of a smooth PPTA fiber (left) and a PPTA fiber with defects (right).

However, despite the relatively low tensile strengths and difficult spinning conditions compared to conventional *p*-aramid fiber, this work for the first time reported high-performance electrospun *p*-aramid fibers from anisotropic solutions. Moreover, it showed the potential of rigid (or semi-rigid) rod polymers for achieving high mechanical performance in electrospun fibers.

4. Conclusion

In this work, the electro-spinnability of isotropic PPTA solutions and anisotropic PPTA solutions has been evaluated. Fibers could be fabricated from all anisotropic solutions by adjusting spinning parameters but only droplets and short fibers were obtained from isotropic solutions. Spinning of the anisotropic PPTA solutions gave numerous secondary solution jets and fiber branches and resulted in a broad diameter distribution in as-spun fibers. The smallest diameter fibers in these branched PPTA fibers showed significantly higher mechanical properties with values of tensile strength and Young's modulus of 1.1 and 59 GPa for fibers with a diameter of 2.1 μm. A geometrical model based on a reduction for the size-dependent Young's modulus was developed to predict the properties of the fibers.

It is, however, worth reminding that the electrospinning process in this research work is difficult to control due to the fiber branching as a result from the high voltage applied. Moreover, only small quantities of electrospun *p*-aramid fiber could be collected. However, the work did report for the first time report the use of anisotropic solutions for the electrospinning of PPTA fibers, while at the same time showing the potential of achieving high levels of property improvement in electrospun fibers using rigid (or semi-rigid) rod polymers. The maximum properties achieved in this work are among the highest reported for electrospun fibers and approach those of commercial *p*-aramid fibers.

Acknowledgements: We are grateful to Teijin Aramid for the supply of PPTA solutions. We thank Dr. Zofia Luklinska for her help on SEM.

Received: April 7, 2015; Revised: June 9, 2015; Published online: July 21, 2015; DOI: 10.1002/mame.201500130

Keywords: anisotropic; electrospinning; mechanical properties; p-aramid; size-effect

[1] J. Yao, C. W. Bastiaansen, T. Peijs, *Fibers* **2014**, *2*, 158.
[2] A. Greiner, J. H. Wendorff, *Angew. Chem. Int. Ed.* **2007**, *46*, 5670.
[3] A. Greiner, J. H. Wendorff, in *Self-Assembled Nanomaterials I*, T. Shimizu, Eds., Springer Berlin Heidelberg, Berlin, Germany **2008**, p. 107.
[4] C. Huang, S. Chen, D. H. Reneker, C. Lai, H. Hou, *Adv. Mater.* **2006**, *18*, 668.
[5] a) X. Zong, S. Ran, D. Fang, B. S. Hsiao, B. Chu, *Polymer* **2003**, *44*, 4959; b) S. Z. Wu, X. P. Yang, F. Zhang, X. X. Hou, *Adv. Mater. Res.* **2008**, *47*, 1169.
[6] H. Yang, *Kevlar Aramid Fiber*, John Wiley & Sons, Chichester, NH, USA **1993**.
[7] a) S. L. Kwolek, P. W. Morgan, J. Schaefgen, L. Gulrich, *Macromolecules* **1977**, *10*, 1390; b) P. W. Morgan, S. L. Kwolek, T. C. Pletcher, *Macromolecules* **1987**, *20*, 729.
[8] a) M. Dobb, D. Johnson, B. Saville, *J. Polym. Sci.: Polym. Phys. Ed.* **1977**, *15*, 2201; b) T. Bair, P. W. Morgan, F. Killian, *Macromolecules* **1977**, *10*, 1396.
[9] G. Srinivasan, D. H. Reneker, *Polym. Int.* **1995**, *36*, 195.
[10] E. Lepore, A. Marchioro, M. Isaia, M. J. Buehler, N. M. Pugno, *PloS ONE* **2012**, *7*, e30500.
[11] a) M. Lewin, *Handbook of Fiber Chemistry*, 3rd edition, Taylor & Francis Group, Boca Raton, FL, USA **2006**, p. 812. b) J. W. Hearle, *High-Performance Fibres*, Woodhead Publishing, Cambridge, England **2001**, p. 93.
[12] S. Ramakrishna, *An Introduction to Electrospinning and Nanofibers*, World Scientific Publishing Co. Pte. Ltd, Singapore **2005**, p. 90.
[13] a) H. E. Darling, *J. Chem. Eng. Data.* **1964**, *9*, 421; b) R. E. Bolz, *CRC Handbook of Tables for Applied Engineering Science*, Chemistry Rubber Company, Boca Raton, FL **1973**, p. 93.
[14] J. H. Wendorff, S. Agarwal, A. Greiner, *Electrospinning: Materials, Processing, and Applications*, John Wiley & Sons, Weinheim, Germany **2012**, p. 69.
[15] a) E. Tan, C. Lim, *Appl. Phys. Lett.* **2004**, *84*, 1603; b) C. Lim, E. Tan, S. Ng, *Appl. Phys. Lett.* **2008**, *92*, 141908; c) C. A. Bashur, L. A. Dahlgren, A. S. Goldstein, *Biomaterials* **2006**, *27*, 5681; d) C.-L. Pai, M. C. Boyce, G. C. Rutledge, *Polymer* **2011**, *52*, 2295; e) S. Y. Chew, T. C. Hufnagel, C. T. Lim, K. W. Leong, *Nanotechnology* **2006**, *17*, 3880; f) M. K. Shin, S. I. Kim, S. J. Kim, S.-K. Kim, H. Lee, G. M. Spinks, *Appl. Phys. Lett.* **2006**, *89*, 231923; g) S. F. Fennessey, R. J. Farris, *Polymer* **2004**, *45*, 4217.
[16] A. Arinstein, M. Burman, O. Gendelman, E. Zussman, *Nat. Nanotechnol.* **2007**, *2*, 59.
[17] A. Ajji, P. Coates, M. Dumoulin, I. Ward, *Solid Phase Processing of Polymers*, Carl Hanser Verlag, Munich, Germany **2000**, p. 85.
[18] a) M. Northolt, *Polymer* **1980**, *21*, 1199; b) M. Northolt, J. Van Aartsen, *J. Polym. Sci., Polym. Symp.* **1977**, *58*, 283.